Design and Modelling of 1 kW, 200–400 V, Multiphase Boost Converter

A. Soubhagya, Ravikiran Rao M, and Suryanarayana K.

1 Introduction

Many high-power applications require boost converters as an integral interface between the available low voltage sources and the output loads, which operate at higher voltages. Based on the type of application, either single-phase or multiphase boost converters are used. In single-phase boost converter for higher power applications, voltage and current stress on the switch increases, and also, voltage and current ripples in the output and input side increase leading to huge filter requirement and increased EMI issues. As a result, losses in the system increase causing poor efficiency and higher cost. This issue can be solved by increasing the number of phases (multiphase topology), which divides the current according to the number of phases and reduces the stress on switches and ripples in the input and output parameters.

Silicon switches suffer from drawbacks such as low bandgap energy, switching frequency limitations and low thermal conductivity. Wide bandgap semiconductors, such as silicon carbide (SiC) and gallium nitride (GaN), provide larger bandgaps, higher breakdown electric field and higher thermal conductivity. SiC switches provide higher blocking voltage, higher junction temperature and higher switching frequencies while compared to Si switches [1]. Operation of the system at higher switching frequency reduces the size of passive components required in the converter, and size of heat sink required will be less because of higher thermal conductivity [2].

A. Soubhagya (✉) · Ravikiran Rao M · Suryanarayana K.
Department of Electrical and Electronics Engineering, NMAM Institute of Technology, Nitte, Karkala, India

Ravikiran Rao M
e-mail: ravikiranraom@nitte.edu.in

Suryanarayana K.
e-mail: suryanarayana@nitte.edu.in

Sanjeevikumar et al. (eds.), *Advances in Renewable Energy and Electric Vehicles*,
Lecture Notes in Electrical Engineering 767,
https://doi.org/10.1007/978-981-16-1642-6_10

In this paper, a 1 kW, 200–400 V, multiphase boost converter which is quite suitable to use in electric vehicles, battery charging, motor drivers, PV systems, etc., is designed and modelled, and the improved efficiency and reliability of the system due to SiC switch are also observed. The main focus is on reducing the ripples, losses and cost of the system. The PWM signals and control algorithms required for the converter are generated using the microcontroller MC56F84789. It has a full set of programmable peripherals such as PWM, ADC, DAC and timers [3].

Section 2 presents the design parameters and conditions of the system and also the reasons to choose multiphase topology. Sections 3 and 4 present state space modelling and small signal analysis, respectively, and also arrive at the transfer function of the converter. Controller design conditions and calculation of parameters are shown in Sect. 5. The simulation and hardware implementation of the system are presented in Sects. 6 and 7, respectively. Section 8 presents the conclusion about the converter and results.

2 System Overview

The system under consideration is a 200–400 V, 1 kW boost converter. To achieve the desired goal of highly efficient and reliable system, a boost converter will be developed using SiC devices which will help in improving the system efficiency. Desired control signals will be generated using in-house developed control card that houses NXP make MC56F84789 controller. The signals from controller are fed to a driver board which houses driver IXDN609SI IC. The input power and necessary isolated power supply are generated from 100 to 300 V flyback SMPS designed in-house. The block diagram of the proposed converter is shown in Fig. 1. To achieve rugged and stable operation of the system, voltage and current at input and output are continuously monitored using signal conditioning units and Hall effect sensors. These feedback signals help to achieve complete control of the system and also to regulate the output to desired value by generating appropriate PWM signals.

Employing multiphase provides advantages that include

1. Thermal performance related to conduction losses of the power supply is proportional to square of current. If multiple phases are used, these losses can be reduced.
2. The system will be more compact in size.
3. Ripple current cancellation
4. Improved transient response
5. Optimized efficiency over the load range
6. Lower output ripple voltage [4].

The design requirements are as in Table 1.

The calculated values of the components /parameters of the system are shown in Table 2 [5, 6].

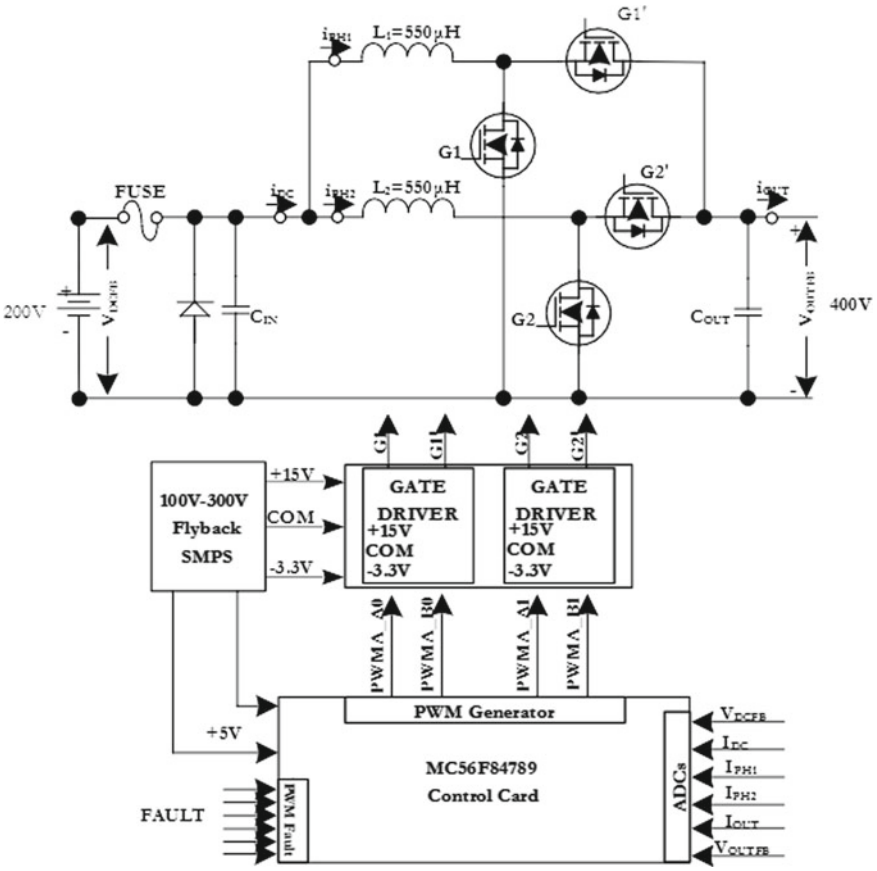

Fig. 1 Block diagram of the system

Table 1 Design parameters of the converter

Sl.No	Parameter	Description	Value
1	V_{in}	Input voltage	200 V
2	V_{out}	Output voltage	400 V
3	P_o	Output power	1 kW
4	f_s	Switching frequency	100 kHz
5	η	Efficiency (assumed)	95%
6	ΔI	Ripple current (assumed)	30%

3 State Space Model

An efficient mathematical modelling of the system plays a crucial role in optimal and accurate design of the controller.

Table 2 Values of components/parameters of the converter

Sl. No.	Parameters	Equation	Value
1	Duty cycle	$D = 1 - \frac{\eta * V_{in}}{V_o}$	0.5725
2	Input current	$I_{in} = \frac{P_o}{\eta * V_o}$	5.84 A
3	Average current per phase	$I_{ph} = \frac{I_{in}}{2}$	2.92 A
4	Inductor per phase	$L = \frac{V_i * D}{\Delta I * f_s}$	555 µH
5	Capacitor	$C = \frac{V_o^* D}{\Delta V^* R_L^* 2^* f_s}$	10 µF
6	Resistor	$R_L = \frac{V_o^2}{P_o}$	160 Ω

It is clear that there is a strong need for a fast and accurate model that can tackle the many difficult design trade-offs and also ensure accuracy at the limits. One such method is state space modelling.

3.1 Single-Phase Boost Converter

Consider the boost converter circuit shown in Fig. 2 with source voltage v_g, source current i_g, capacitor current i_c, capacitor voltage v_c, output voltage v_o and output current i_o.

Let the state variables be inductor current i_L and capacitor voltage v_c and output variables be v_o and i_c [7–10].

When the switch S is in ON condition,

$$L\frac{\mathrm{d}i_L(t)}{\mathrm{d}t} = v_g \tag{1}$$

$$C\frac{\mathrm{d}v_c(t)}{\mathrm{d}t} + \frac{v_c}{R} + i_0 = 0 \tag{2}$$

Rearranging Eqs. 1 and 2,

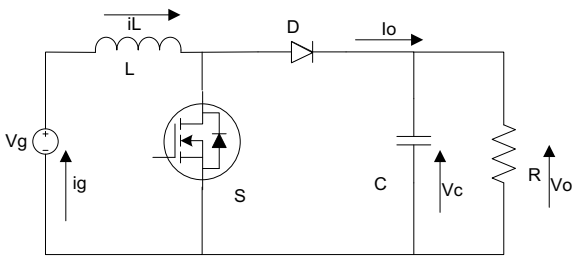

Fig. 2 Single-phase boost converter circuit

$$\frac{\mathrm{d}i_L(t)}{\mathrm{d}t} = \frac{v_g}{L} \tag{3}$$

$$\frac{\mathrm{d}v_c(t)}{\mathrm{d}t} = -\frac{v_c}{RC} - \frac{i_0}{C} \tag{4}$$

Arranging the Eqs. 3 and 4,

$$\begin{bmatrix} \frac{\mathrm{d}i_L(t)}{\mathrm{d}t} \\ \frac{\mathrm{d}v_c(t)}{\mathrm{d}t} \end{bmatrix} = \begin{bmatrix} 0 & 0 \\ 0 & -1/RC \end{bmatrix} \begin{bmatrix} i_L \\ v_c \end{bmatrix} + \begin{bmatrix} 1/L \\ 0 \end{bmatrix} v_g + \begin{bmatrix} 0 \\ -1/C \end{bmatrix} \tag{5}$$

When the switch is in OFF condition,

$$L\frac{\mathrm{d}i_L(t)}{\mathrm{d}t} = v_g - v_c \tag{6}$$

$$C\frac{\mathrm{d}v_c(t)}{\mathrm{d}t} + \frac{v_c}{R} + i_0 - i_L = 0 \tag{7}$$

Rearranging Eqs. 6 and 7,

$$\begin{bmatrix} \frac{\mathrm{d}i_L(t)}{\mathrm{d}t} \\ \frac{\mathrm{d}v_c(t)}{\mathrm{d}t} \end{bmatrix} = \begin{bmatrix} 0 & -1/L \\ -1/C & -1/RC \end{bmatrix} \begin{bmatrix} i_L \\ v_c \end{bmatrix} + \begin{bmatrix} 1/L \\ 0 \end{bmatrix} v_g + \begin{bmatrix} 0 \\ -1/C \end{bmatrix} i_0 \tag{8}$$

The output equations during ON and OFF conditions can be, respectively, written as

$$\begin{matrix} v_o \\ i_g \end{matrix} = \begin{pmatrix} 0 & 1 \\ 1 & 0 \end{pmatrix} \begin{matrix} i_L \\ v_c \end{matrix} \tag{9}$$

Equations 5 and 8 are in the form

$$\frac{\mathrm{d}x(t)}{\mathrm{d}t} = Ax(t) + Bu(t)$$

And Eq. 9 in the form

$$y(t) = Cx(t) + Eu(t)$$

Therefore, to obtain the final form,

$$\begin{aligned} A &= A_1 d + A_2(1-d) \\ B &= B_1 d + B_2(1-d) \\ C &= C_1 d + C_2(1-d) \\ E &= E_1 d + E_2(1-d) \end{aligned}$$

where d is the duty ratio of the converter.
By substituting the values, the state space equation can be written as

$$\begin{bmatrix} \frac{di_L(t)}{dt} \\ \frac{dv_c(t)}{dt} \end{bmatrix} = \begin{bmatrix} 0 & \frac{-(1-d)}{C} \\ \frac{(1-d)}{C} & -1/RC \end{bmatrix} \begin{matrix} i_L \\ v_c \end{matrix} + \begin{bmatrix} \frac{1}{L} \\ 0 \end{bmatrix} v_g + \begin{bmatrix} 0 \\ \frac{1}{-C} \end{bmatrix} i_0 \tag{10}$$

This equation is also known as average large signal model.
The output equation remains the same as shown in Eq. (9), since $E = 0$.

3.2 Multiphase Boost Converter

Consider the multiphase boost converter circuit shown in Fig. 3 with source voltage v_g, source current i_g, capacitor current i_c, capacitor voltage v_c, output voltage v_o and output current i_o. Let the state variables be capacitor voltage v_c and inductor currents of phase 1 and 2, i.e. $i_{L1,}$ $i_{L2,}$ respectively, and output variables be v_o and i_c [7–10].

The operation of two-phase boost converter can be divided into four modes. Consider the state space variables similar to used in single-phase boost converter.

(1) *Mode 1*

When switch $S1$ is in ON condition and Mode 12 is in OFF condition,

$$L_1 \frac{di_{L1}(t)}{dt} = v_g \tag{11}$$

Since Mode 12 is in OFF position,

$$L_2 \frac{di_{L2}(t)}{dt} = v_c \tag{12}$$

$$i_{L2} = C \frac{dv_c(t)}{dt} + \frac{v_c}{R} \tag{13}$$

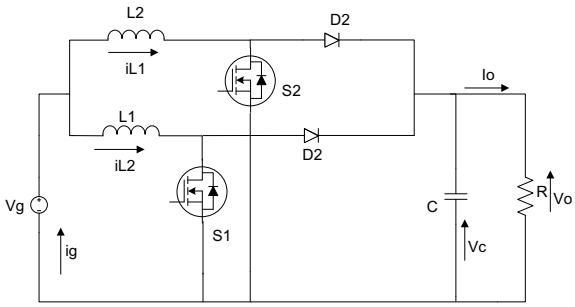

Fig. 3 Multiphase boost converter circuit

$$\frac{\mathrm{d}v_c(t)}{\mathrm{d}t} = \frac{i_{L2}}{C} - \frac{v_c}{RC} \tag{14}$$

(2) *Mode 2*

When both the switches $S1$ and $S2$ are in OFF condition,

$$L_1 \frac{\mathrm{d}i_{L1}(t)}{\mathrm{d}t} = v_c \tag{15}$$

$$L_2 \frac{\mathrm{d}i_{L2}(t)}{\mathrm{d}t} = v_c \tag{16}$$

$$i_{L1} + i_{L2} = C \frac{\mathrm{d}v_c(t)}{\mathrm{d}t} + \frac{v_c}{R} \tag{17}$$

(3) *Mode 3*

When switch $S1$ is in ON condition and $S2$ is in OFF condition,

$$L_2 \frac{\mathrm{d}i_{L2}(t)}{\mathrm{d}t} = v_g \tag{18}$$

Since $S1$ is in OFF condition,

$$L_1 \frac{\mathrm{d}i_{L1}(t)}{\mathrm{d}t} = v_c \tag{19}$$

$$i_{L1} = C \frac{\mathrm{d}v_c(t)}{\mathrm{d}t} + \frac{v_c}{R} \tag{20}$$

$$\frac{\mathrm{d}v_c(t)}{\mathrm{d}t} = \frac{i_{L1}}{C} - \frac{v_c}{R} \tag{21}$$

(4) *Mode 4*

It follows the same procedure as of mode 2 resulting in same set of equations. Mode 1 can be rearranged and written as

$$\begin{bmatrix} \frac{\mathrm{d}i_{L1}(t)}{\mathrm{d}t} \\ \frac{\mathrm{d}i_{L2}(t)}{\mathrm{d}t} \\ \frac{\mathrm{d}v_c(t)}{\mathrm{d}t} \end{bmatrix} = \begin{bmatrix} 0 & 0 & 0 \\ 0 & 0 & 1/L2 \\ 0 & 1/C & -1/RC \end{bmatrix} \begin{bmatrix} i_{L1} \\ i_{L2} \\ v_c \end{bmatrix} + \begin{bmatrix} 1/L1 \\ 0 \\ 0 \end{bmatrix} v_g + \begin{bmatrix} 0 \\ 0 \\ 1/C \end{bmatrix} i_0 \tag{22}$$

Mode 2 and Mode 4 can be written as

$$\begin{bmatrix} \frac{\mathrm{d}i_{L1}(t)}{\mathrm{d}t} \\ \frac{\mathrm{d}i_{L2}(t)}{Et} \\ \frac{\mathrm{d}v_c(t)}{\mathrm{d}t} \end{bmatrix} = \begin{bmatrix} 0 & 0 & 1/L1 \\ 0 & 0 & 1/L2 \\ 0 & 0 & -1/RC \end{bmatrix} \begin{bmatrix} i_{L1} \\ i_{L2} \\ v_c \end{bmatrix} + \begin{bmatrix} 0 \\ 0 \\ 0 \end{bmatrix} v_g + \begin{bmatrix} 0 \\ 0 \\ 1/C \end{bmatrix} i_0 \tag{23}$$

Mode 3 can be written as

$$\begin{bmatrix} \frac{di_{L1}(t)}{dt} \\ \frac{di_{L2}(t)}{dt} \\ \frac{dv_c(t)}{dt} \end{bmatrix} = \begin{bmatrix} 0 & 0 & 1/L1 \\ 0 & 0 & 0 \\ 1/C & 0 & -1/RC \end{bmatrix} \begin{bmatrix} i_{L1} \\ i_{L2} \\ v_c \end{bmatrix} + \begin{bmatrix} 0 \\ 1/L2 \\ 0 \end{bmatrix} v_g + \begin{bmatrix} 0 \\ 0 \\ 1/L1 \end{bmatrix} i_0 \quad (24)$$

To obtain the complete state space matrix, by referring to Eqs. (22), (23), (24).

$$\text{We have } A1 = \begin{bmatrix} 0 & 0 & 0 \\ 0 & 0 & 1/L2 \\ 0 & 1/C & -1/RC \end{bmatrix}$$

$$A2 = A4 = \begin{bmatrix} 0 & 0 & 1/L1 \\ 0 & 0 & 1/L2 \\ 0 & 0 & -1/RC \end{bmatrix}, \; A3 = \begin{bmatrix} 0 & 0 & 1/L1 \\ 0 & 0 & 1/L2 \\ 0 & 0 & -1/RC \end{bmatrix}$$

$$B1 = \begin{bmatrix} 1/L1 \\ 0 \\ 0 \end{bmatrix} B2 = B4 = \begin{bmatrix} 0 \\ 0 \\ 0 \end{bmatrix}, B3 = \begin{bmatrix} 0 \\ 1/L2 \\ 0 \end{bmatrix}$$

Therefore,

$$A = A_1 d_1 + A_2 d_2 + A_3 d_3 + A_4 d_4$$
$$B = B_1 d_1 + B_2 d_2 + B_3 d_3 + B_4 d_4$$

d_1, d_2, d_3, d_4 are duty ratio in mode 1, mode 2, mode 3, mode 4, respectively. By substituting respective values

$$\begin{bmatrix} \frac{di_{L1}(t)}{dt} \\ \frac{di_{L2}(t)}{dt} \\ \frac{dv_c(t)}{dt} \end{bmatrix} = \begin{bmatrix} 0 & 0 & \frac{(1-d_1)}{L1} \\ 0 & 0 & \frac{(1-d_3)}{L2} \\ \frac{(1-d_1)}{C} & \frac{(1-d_3)}{C} & -1/RC \end{bmatrix} \begin{bmatrix} i_{L1} \\ i_{L2} \\ v_c \end{bmatrix} + \begin{bmatrix} \frac{d_1}{L1} \\ \frac{d_3}{L2} \\ 0 \end{bmatrix} v_g + \begin{bmatrix} 0 \\ 0 \\ 1/C \end{bmatrix} i_0 \quad (25)$$

4 Small Signal Model

For single-phase boost converter, at the equilibrium condition, $\frac{dx(t)}{dt} = 0, d = D, v_g = V_g, i_g = I_g$, accordingly [10].
Therefore, Eq. (10) becomes

$$\begin{matrix} 0 \\ 0 \end{matrix} = \begin{pmatrix} 0 & \frac{-(1-D)}{C} \\ \frac{(1-D)}{C} & -1/RC \end{pmatrix} \begin{matrix} I_L \\ V_c \end{matrix} + \begin{matrix} \frac{1}{L} \\ 0 \end{matrix} V_g + \begin{matrix} 0 \\ \frac{1}{-C} \end{matrix} I_0 \quad (26)$$

This is in the form of

$$AX + BU = 0$$

Small signal model is obtained by substituting in average large signal model, for every variable a steady state part and a small signal variation about the equilibrium point,

i.e.

$$\begin{aligned} d &= D + d^{\wedge} \\ v_o &= V_o + v_o^{\wedge} \\ v_g &= V_g + v_g^{\wedge} \\ i_o &= I_o + i_o^{\wedge} \\ i_L &= I_L + i_L^{\wedge} \end{aligned}$$

Since $AX + BU = 0$ at equilibrium, Eq. 10 can be written as

$$\begin{pmatrix} \frac{\mathrm{d}i_L^{\wedge}(t)}{\mathrm{d}t} \\ \frac{\mathrm{d}v_c^{\wedge}(t)}{\mathrm{d}t} \end{pmatrix} = \begin{pmatrix} 0 & \frac{-(1-D-d^{\wedge})}{C} \\ \frac{(1-D-d^{\wedge})}{C} & -1/RC \end{pmatrix} \begin{matrix} I_L + i_L^{\wedge} \\ V_c + v_c^{\wedge} \end{matrix} + \begin{matrix} \frac{1}{L} \\ 0 \end{matrix} (V_g + v_g^{\wedge}) + \begin{matrix} 0 \\ \frac{1}{-C} \end{matrix} \left(I_o + i_o^{\wedge}\right) \quad (27)$$

By simplification,

$$\begin{pmatrix} \frac{\mathrm{d}i_L^{\wedge}(t)}{\mathrm{d}t} \\ \frac{\mathrm{d}v_c^{\wedge}(t)}{\mathrm{d}t} \end{pmatrix} = \begin{pmatrix} 0 & \frac{-(1-D)}{C} \\ \frac{(1-D)}{C} & -1/RC \end{pmatrix} \begin{matrix} i_L^{\wedge} \\ v_c^{\wedge} \end{matrix} + \begin{matrix} V_c/L \\ (-I_L)/C \end{matrix} \mathrm{d}^{\wedge} + \begin{matrix} \frac{1}{L} \\ 0 \end{matrix} v_g^{\wedge} + \begin{matrix} 0 \\ \frac{1}{-C} \end{matrix} i_o^{\wedge} \quad (28)$$

Therefore, state equation of small signal model is

$$\begin{pmatrix} \frac{\mathrm{d}i_L^{\wedge}(t)}{\mathrm{d}t} \\ \frac{\mathrm{d}v_c^{\wedge}(t)}{\mathrm{d}t} \end{pmatrix} = \begin{pmatrix} 0 & \frac{-(1-D)}{C} \\ \frac{(1-D)}{C} & -1/RC \end{pmatrix} \begin{matrix} i_L^{\wedge} \\ v_c^{\wedge} \end{matrix} + \begin{matrix} \frac{1}{L} & 0 & V_c/L \\ 0 & \frac{1}{-C} & \frac{(-I_L)}{C} \end{matrix} \begin{matrix} v_g^{\wedge} \\ i_o^{\wedge} \\ \mathrm{d}^{\wedge} \end{matrix} \quad (29)$$

Similarly, for the two-phase boost converter,

$$\begin{bmatrix} \frac{\mathrm{d}i_{L1}^{\wedge}(t)}{\mathrm{d}t} \\ \frac{\mathrm{d}i_{L2}^{\wedge}(t)}{\mathrm{d}t} \\ \frac{\mathrm{d}v_c^{\wedge}(t)}{\mathrm{d}t} \end{bmatrix} = \begin{bmatrix} 0 & 0 & \frac{(1-D_1)}{L1} \\ 0 & 0 & \frac{(1-D_3)}{L2} \\ \frac{(1-D_1)}{C} & \frac{(1-D_3)}{C} & -1/RC \end{bmatrix} \begin{bmatrix} i_{L1}^{\wedge} \\ i_{L2}^{\wedge} \\ v_c^{\wedge} \end{bmatrix} + \begin{bmatrix} \frac{\mathrm{d}_1}{L1} & 0 & V_c/L1 \\ \frac{\mathrm{d}_3}{L2} & 0 & \frac{(-I_{L2})}{C} \\ 0 & 1/C & 0 \end{bmatrix} \begin{bmatrix} v_g^{\wedge} \\ i_o^{\wedge} \\ d^{\wedge} \end{bmatrix} \quad (30)$$

We have state space model given by

$$\dot{x} = Ax + Bu \quad (31)$$

$$y = Cx \tag{32}$$

Taking Laplace transform of the above equations,

$$sX(s) = AX(s) + BU(s) \tag{33}$$

$$Y(s) = CX(s) \tag{34}$$

By further simplification,

$$Y(s) = C(sI - A)^{-1}BU(s) \tag{35}$$

Therefore, by substituting corresponding values from Eqs. (26) and (30), the transfer function of output voltage to duty ratio for both single and multiphase can be obtained as

- Single-phase converter

$$\frac{\hat{v}_o(s)}{\hat{d}(s)} = \frac{D'v_c - sI_L L}{L\left[s^2 + \frac{s}{RC} + D'^2\right]} \tag{36}$$

where $D' = 1-D$.

- Multiphase converter

$$\frac{\hat{v}_o(s)}{\hat{d}(s)} = \frac{RL_1L_2\left[\frac{D_1'*v_c}{L_1} - \frac{D_3'*I_{L2}}{C}\right]s}{s^3L_1L_2 + \left(L_1L_2 - D'^{1^2}RL_2\right)s + RL_1D'^{3^2}} \tag{37}$$

where $D_1' = 1-D_1$ and $D_3' = 1-D_3$.

5 Controller Design

To maintain the constant and stable output of the system, closed loop controllers are employed. Controllers are designed in such a way to regulate the output parameters based on the changes in input and output conditions (Fig. 4).

V_g, V_o, d are the input voltage, output voltage and duty cycle of the system, respectively. The feedback of the parameter to be controlled is taken and compared with the reference value, and this gives error output. The ideal control occurs when there is zero error, but in practical scenario, it is quite impossible [10].

If K is controller gain,v_c is control voltage, then

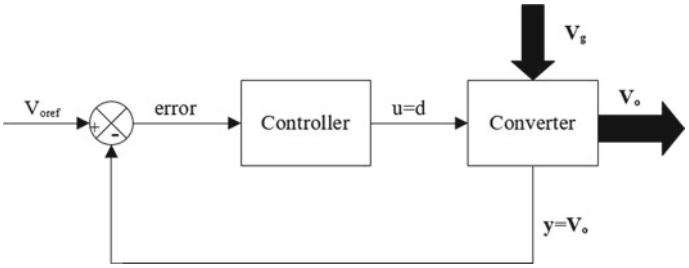

Fig. 4 Block diagram of generic controller

$$\mathrm{e} = \frac{v_c}{K}$$

For $\mathrm{e} = 0$, either $v_c = 0$ or $K =$ infinity. But $v_c = 0$ will result in broken loop, i.e. there will be no enclosed negative feedback resulting in no use of controller. So, to have lesser error value, K should be very high. Therefore, based on K and error value, different types of controllers such as P, I, PI, PD, PID are designed. For the multiphase boost converter under consideration (Sect. 2), a PI controller is designed.

The controller can be designed using different methods.

- Tuning the controller directly on the system (hardware or simulation), also known as Ziegler–Nicholas technique
- By formal approach, i.e. methods such as root locus technique are used to deduce the controller parameters and then included in hardware or simulation. This method is mainly used for non-minimum phase system such as boost converter. Initially, the state space equations and small signal model of the plant are determined. The root locus of the system is found, and the system is tested for satisfactory step response. Later, the values from these calculations are used to determine the controller parameters.

Using a PI controller provides better transient response and nearly zero steady state error. It also has the advantages such as removal of high frequency noise, improved phase margin and gain margin. Thus, for the proposed multiphase boost converter, a PI controller is designed using Ziegler–Nicholas technique.

For PI controller,

$$v_c = K_p + K_i \int e \, \mathrm{d}t$$

where K_p is proportionality scaling factor, and K_i is integrator scaling factor. For tuning the controller,

- Set up the open loop system.
- Introduce limiters across the integrator and v_c. This is done so that v_c swing can fall in sync with that of PWM.

- Keeping the system in open loop, check phase relationship.
  Let $K_i = 0$ and $K_p =$ finite value. Phase relationship is stable if y increases with increase in $V_{\text{oref}}$and decreases with decrease in $V_{\text{oref.}}$
- Now, enable the integration initially with low value by keeping $K_p = 0$. Slowly increase the value, till the system reaches steady state.
- After the system reaches steady state, calculate the value of K_p and K_i.

$$K_p = 0.45 * K_u$$
$$K_i = \frac{K_p}{T_u}$$

where K_u is ultimate gain, and T_u is oscillation period.

6 Simulation

6.1 Simulation of Open Loop System

The simulation is conducted in MATLAB/Simulink, and the circuit is as shown in Fig. 5. The system is designed to have an input voltage of 200 V, with duty ratio of 57.25% and switching frequency of 100 kHz.

The input and output DC currents and the phase currents through inductors shown in Fig. 6, depicts that with two-phase topology shows the ripple at input side is minimum.

Gating sequence of the system is designed such that Q2 pulses are delayed by an angle of 180° with respect to Q1 which results in reduction in the input current ripple (Fig. 7).

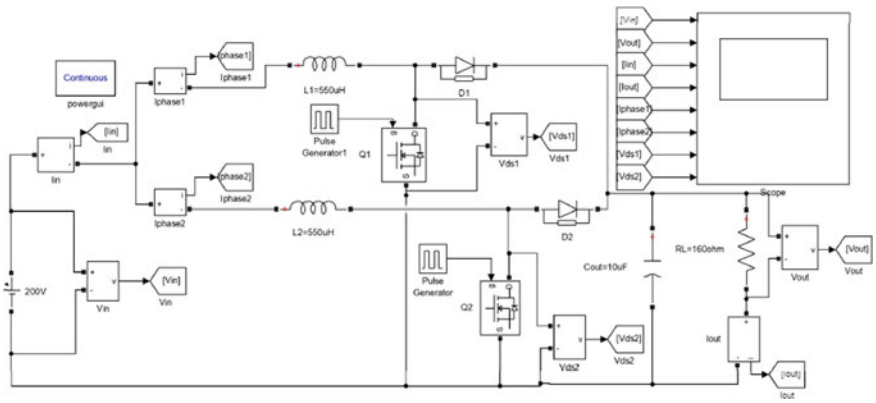

Fig. 5 Simulated circuit of multiphase boost converter (open loop)

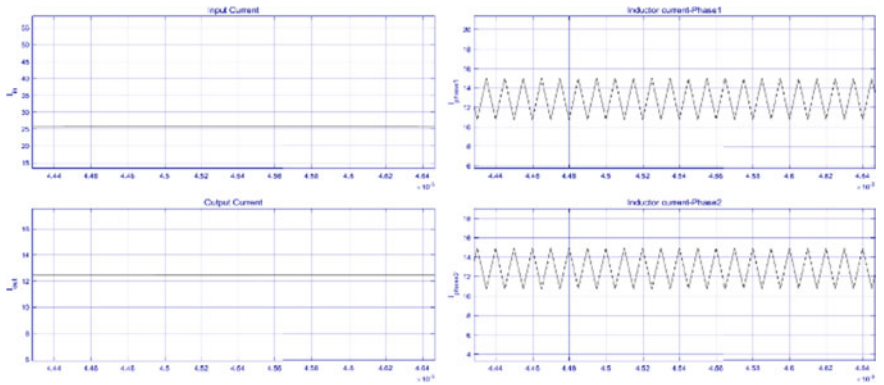

Fig. 6 Current waveforms

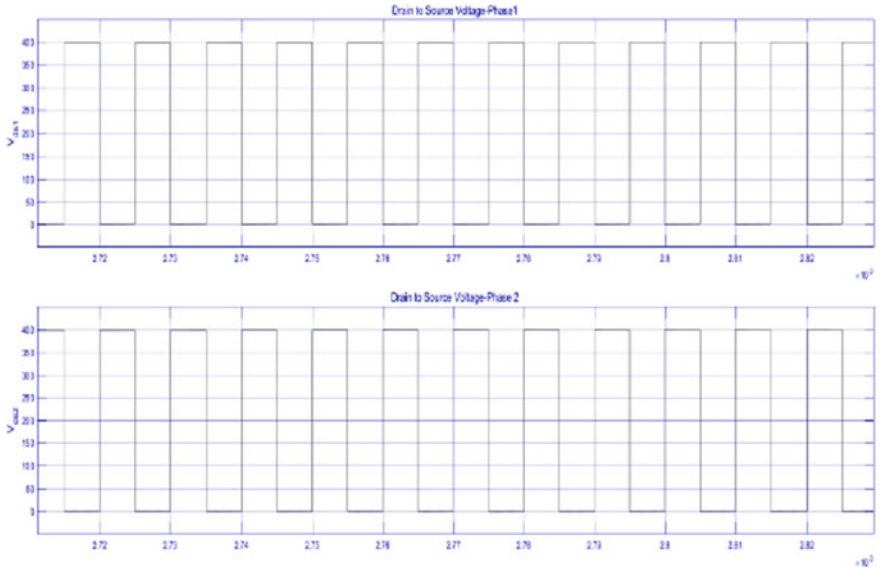

Fig. 7 Drain to source voltages of phase 1 and phase 2

From the results of output voltage, it can also be concluded that output ripples are comparatively less. The output voltage ripple is found to be 1.61% which is in the limits of 1% (Fig. 8).

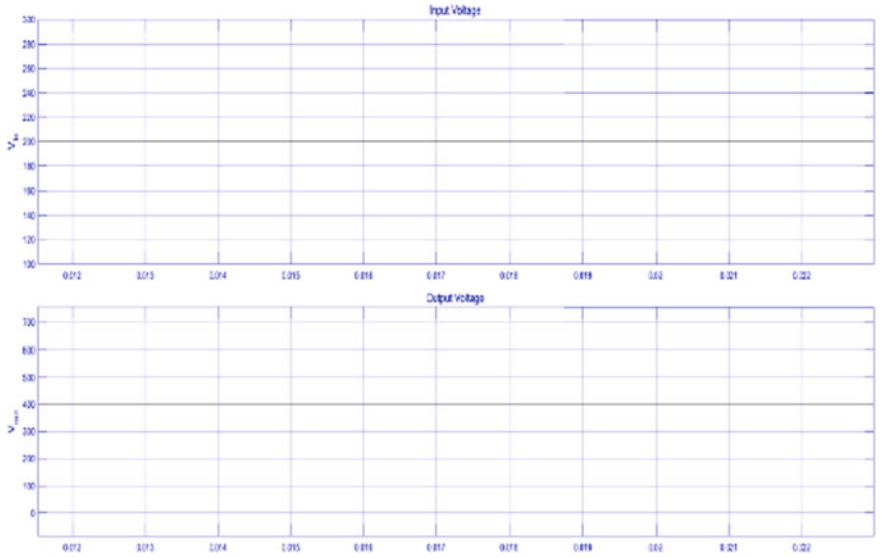

Fig. 8 Input and output voltages

6.2 Simulation of Closed Loop System

For the proposed system, the PI controller is designed using Ziegler–Nicholas technique in Simulink platform. The values of the components used are as mentioned in Sect. 2 (Fig. 9).

As mentioned in Sect. 5, initially K_i is set to zero, and K_p is set to 1 and checked for stability. At $K_p = 1.3$, constant and stable oscillations are obtained as shown in Fig. 10. For this value of K_p, $K_u = 1.3$ and $T_u = 0.001$ s.

The values of K_p and K_i are obtained to be 0.58 and 700, respectively. Figure 11 represents the output voltage of the system, i.e. 400 V.

7 Hardware Implementation

The system is implemented on PCB for higher switching frequency operation by doing schematics followed by layout using OrCad tool. This system is used in an in-house developed electric vehicle for battery charging. The required PWM signals for the switches are provided by the microcontroller MC56F84789. Inherent features such as short circuit protection, protection from inrush current and soft start are implemented. Input to the system can be a DC supply or solar panel. The implemented multiphase boost converter is shown in Fig. 12.

The existing system has been implemented with hysteresis control. The required control signals are generated using MC56F84789, and low pass filter of 40 kHz

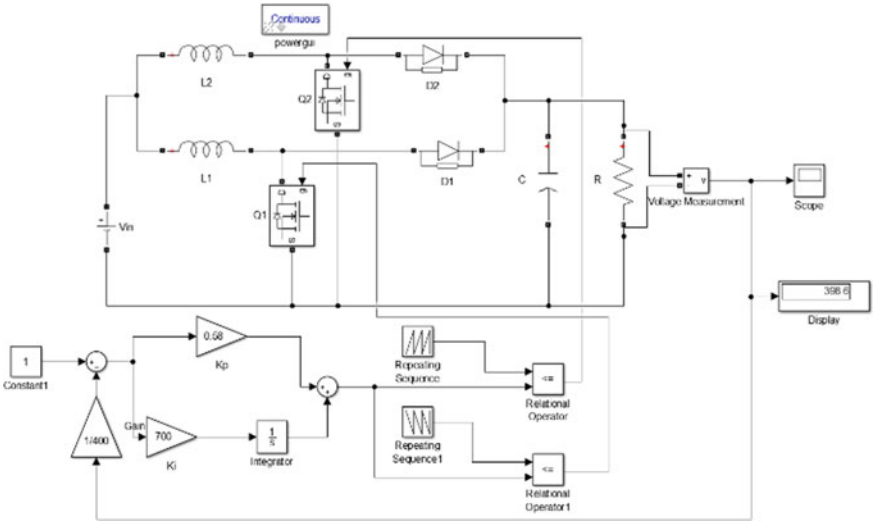

Fig. 9 Simulated model of the system

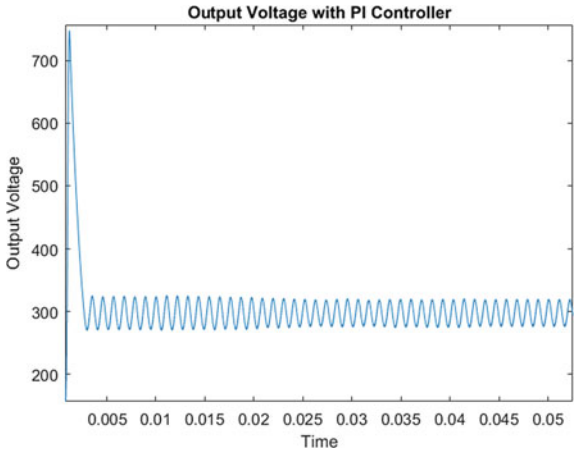

Fig. 10 Output voltage with $K_p = 1.3$, $K_i = 0$

frequency is used for signal conditioning. The output voltage is thus stabilized. Figures 13 and 15 represent the outputs obtained under hysteresis control.

Multiphase topology of the converter is mainly chosen for the reason of reducing ripples in input and output side. It is proven that delaying the sequence of gating pulses by 180° in two-phase converter results in reduction in the input current ripple. This fact is realized both in simulation and practical mode. Figure 14 shows gating pulse, inductor currents in two phases and input current.

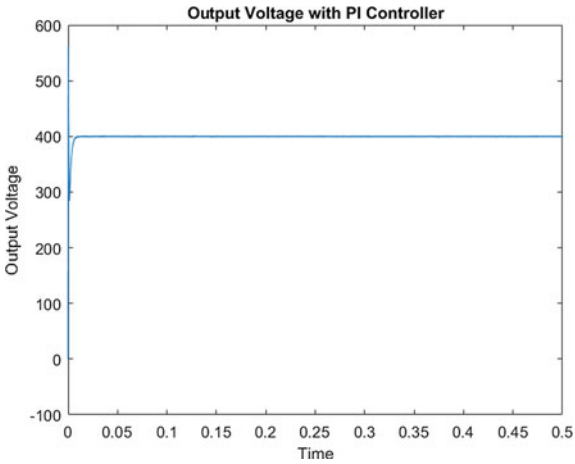

Fig. 11 Output voltage with $K_p = 0.58$, $K_i = 700$

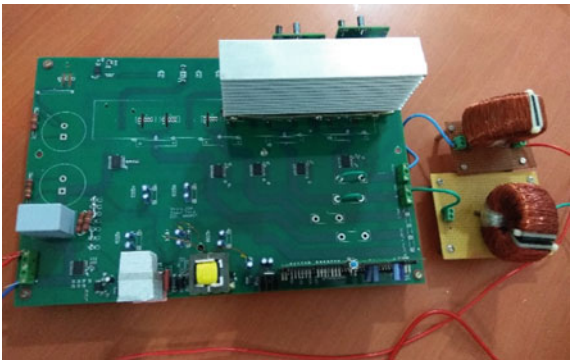

Fig. 12 Implemented multiphase boost converter

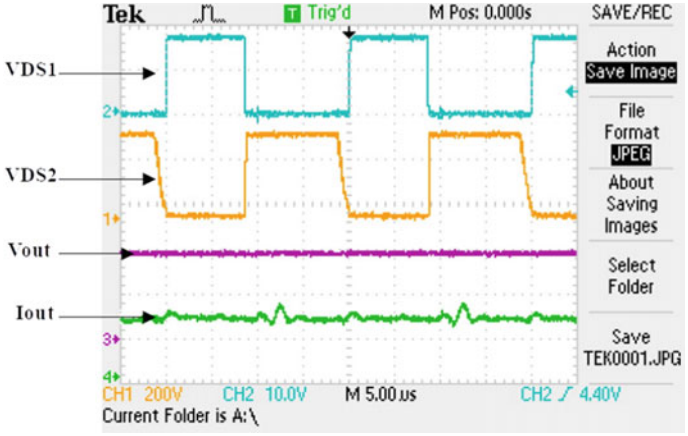

Fig. 13 Converter loaded up to 1 kW with $V_o = 400$ V and $I_o = 2.5$A

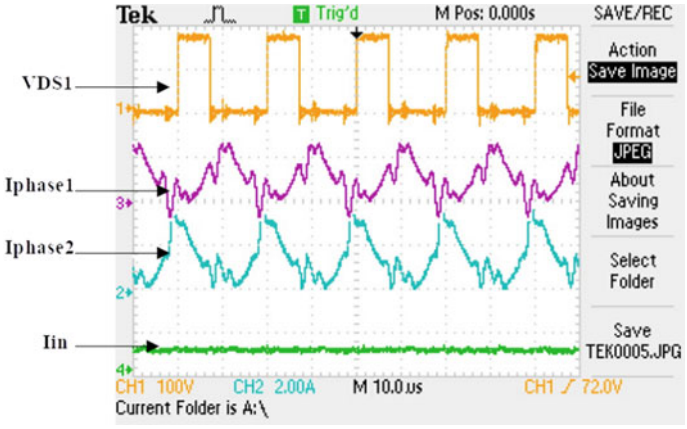

Fig. 14 Boost converter with reduced ripple in input current

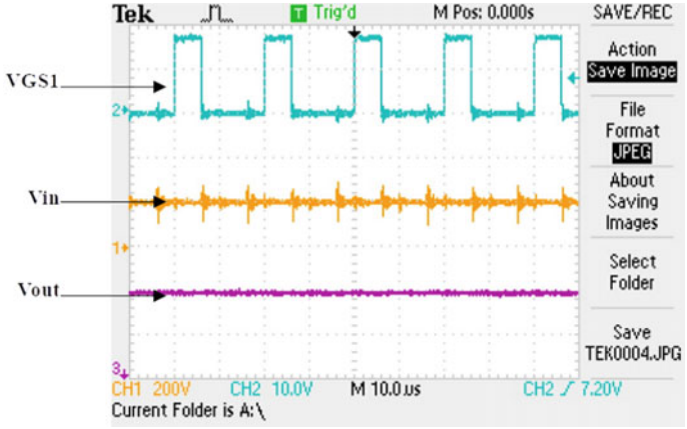

Fig. 15 Light load condition with $V_{in} = 200$ V; $V_{out} = 400$ V

The efficiency of the converter is high during full load condition, and it is low during light load condition. The response of the system during these extreme conditions is observed. Figures 13and15 show system response under full load and light load, respectively.

8 Conclusion

Multiphase boost converter is highly promising for higher current applications with the advantage of reduced ripple current and reduced hot spots on the printed circuit

board. The use of multiphase topology for the proposed boost converter has resulted in the total current getting distributed in different phases and reducing current and thermal stress on the switches. This topology has also reduced the requirement of output filter due to reduced current ripple and higher ripple frequency of the converter.

Usage of SiC switch in the boost converter has considerably reduced the size of the PCB and also usage of heat sinks. The efficiency obtained is high compared to that of a Si switch.

The results from open loop implementation of the converter match with that of the simulation. Hysteresis control has resulted in a stable and efficient output. The designed PI controller for the system has given satisfactory and stable output. Thus, a reliable and stable multiphase boost converter of 1 kW, 200–400 V is designed and implemented meeting all the desired conditions.

Acknowledgements The author would like to thank Dr. Niranjan Chiplunkar, Principal NMAMIT, for always encouraging and supporting the research works. The author would also like to thank 'Centre for Design of Power Electronic Systems' (CDPES), Research and Innovation Centre, NMAMIT.

References

1. A. Elasser, T.P. Chow, Silicon carbide benefits and advantages for power electronics circuits and systems. Proc. IEEE **90**(6), 969–986 (2002). https://doi.org/10.1109/JPROC.2002.1021562
2. G. Vacca, Benefits and advantages of silicon carbide power devices over their silicon counterparts. Semiconductor TODAY Compounds Adv Silicon 12 Issue 3, April/May (2017)
3. Freescale Semiconductor, Inc., "MC56F847xx Reference Manual with Addendum", Document Number: MC56F847XXRM Rev. 2.0, 03/2016
4. Texas Instruments, "AN-1820 LM5032 Interleaved Boost Converter", Application Report SNVA335A–May 2008–Revised May (2013)
5. D.W. Hart, *Power Electronics* (McGraw-Hill, United States, 2001)
6. U. Ned Mohan, in *Power Electronics*, (2nd ed., New York, Wiley inc) (1989)
7. Texas Instruments, Voltage Mode Boost Converter Small Signal Control Loop Analysis Using the TPS61030. SLVA274A–May 2007–Revised January (2009)
8. B. Surya Prabha, S. Ramprasanth, Mathematical modelling and performance analysis of quadratic boost converter. Int. J. Sci. Eng. Res. **9**(3) (2018)
9. P. Tyagi, V.C. Kotak, B. Mathew, V.P. Sunder Singh, State space modelling of high gain DC-DC boost converter with coupling inductor. Int. J. Eng. Res. Technol. (IJERT) **03**(01) (2014)
10. R.W. Erickson, *Fundamentals of Power Electronics* (Kluwer Academic/Plenum Publishers, New York, 2001)